

Anomalous thermalization by dissipation in quantum XY model

Shun-Yao Zhang,¹ Ming Gong,^{1,2,3,*} Guang-Can Guo,^{1,2,3} and Zheng-Wei Zhou^{1,2,3,†}

¹CAS Key Laboratory of Quantum Information, University of Science and Technology of China, Hefei, 230026, Peoples Republic of China

²Synergetic Innovation Center of Quantum Information and Quantum Physics, University of Science and Technology of China, Hefei, Anhui 230026, China

³CAS Center For Excellence in Quantum Information and Quantum Physics

(Dated: May 16, 2022)

We consider the dynamics in the quantum XY model with boundary dissipation. This model after fermionization gives the topological p -wave superconducting model with two localized edge modes at the two ends separated from the bulk spectra by a finite energy gap. The dissipation can induce coupling between the ground states manifold and all the excited bands, which induces thermalization in a characteristic time T^* . In the long time limit, the density matrix will approach the maximal mixed state in each even and odd parity subspaces, with thermalization determined by the single particle dynamics. We find that the thermalization time $T^* \propto N^3/\gamma$ in the weak dissipation limit, where N is the chain length and γ is the dissipation rate; while in the strong dissipation limit, $T^* \propto \gamma N^3$. These analytical results are counterintuitive because it means weak dissipation can induce strong thermalization, while strong dissipation can induce weak thermalization. We find that these two limits correspond to two different physics, which are explained by mapping the single fermion dynamics to a non-Hermitian model. Even in the long chain limit, the dissipation will exhibit strong odd-even effect from the oscillation of wave function at the two ends. These results shade new insight into the dynamics of topological qubits and their stabilities in environment.

While the dynamics of qubits in environment has been well studied [1, 2], the same issue in the many-body systems is still one major challenge in theories [3–11] due to more expensive computation cost [12]. However, this is an important question at least from two diverse aspects. The many-body systems may possess some features that are totally different from the single particle systems, such as ergodicity and thermalization [13, 14], which are fundamental concepts in statistics. In the trapped ions, it may exhibit different dynamics depending strongly on the initial states, which are explained based on quantum many-body scar [15–17]. Moreover, it is also an important issue in topological quantum computation [18–20], in which the two ground states are separated from the excited bands by a finite energy gap. Thus if the temperature is much lower than the excitation gap, the occupation of the excited states are exponentially small. This picture is not necessarily true since any weak dissipation can induce coupling between ground states and excited states. This is a pressing issue in regarding of the possible signatures of Majorana zero modes (MZMs) realized in experiments [21–29]; see reviews in [30, 31].

In this work, we consider the dynamics in the quantum XY spin model with boundary dissipation. This spin model after fermionization can be mapped to the topological p -wave superconducting model [32], thus the two ground states are protected by a finite energy gap. (I) We find that while dissipation plays weak role in direct coupling between the two edge modes, it induces direct coupling between the ground states and all the excited states, leading to thermalization characterized by a typical time scale T^* . (II) We find that in the long time limit, the many-body thermalization is dominated by the

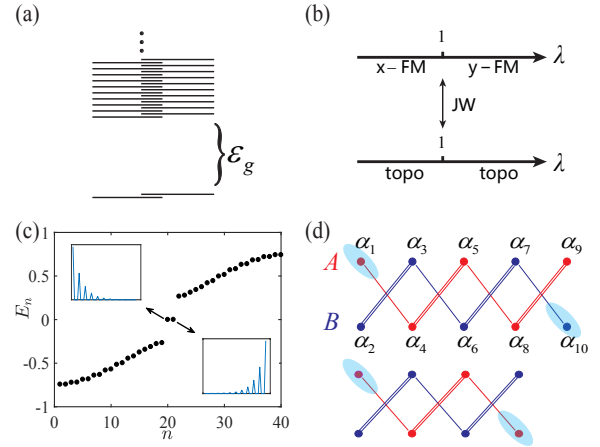


FIG. 1. (a) Energy levels in the XY chain. The two lowest energy levels are separated from the excited bands by a finite energy gap ϵ_g . (b) The two ferromagnetic (FM) phases in the XY model will be mapped to two distinct topological p -wave superconducting phases after Jordan-Wigner (JW) transformation. (c) Energy levels in the fermion representation, in which the two edge modes, occupied or unoccupied, give the two lowest energy levels in the XY model. (d) The odd-even effect in a finite chain due to the oscillation of coupling between the two edge modes in the two chains A and B.

single fermion thermalization process. In the weak dissipation limit, $T^* \propto N^3/\gamma$, where N is the total chain length and γ is the boundary dissipation rate. However, in the strong dissipation limit, $T^* \propto \gamma N^3$. These results are counterintuitive because it means that weak dissipation can induce fast thermalization, while strong dissipation can induce weak thermalization. We under-

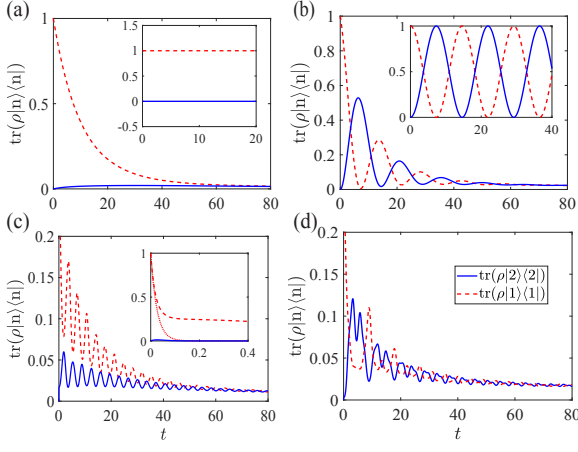


FIG. 2. Evolution in the ground subspace of the quantum XY model. (a) and (b) Evolution of $\text{Tr}(\rho|i\rangle\langle i|)$ for chain $N = 7$ and $N = 6$ with $g_1 = 1, g_2 = 0.7$ and $\gamma = 0.05$. The insets show the evolution without dissipation. (c) and (d) The same evolution for chain $N = 7$ and $N = 6$ with $g_1 = 1, g_2 = 0.7$ and $\gamma = 20$, and the inset (solid line) shows this evolution by neglecting the contribution from all the excited states.

stand these results by mapping the single particle dynamics to a non-Hermitian model. (III) This dynamics exhibits strong odd-even effect in the weak dissipation limit, which reduces to a unified form in the strong dissipation limit. This effect arises from the overlap between the edge modes and the extended modes. These results shade new insight into the dissipation of the topological qubits immersed in environment.

Model and Master Equation. We consider a quantum XY model with boundary dissipation, which can be written as

$$\frac{d\rho}{dt} = \mathcal{L}(\rho) = -i[H, \rho] + \mathcal{D}(\rho). \quad (1)$$

Here $H = -\sum_{i=1}^{N-1} (g_1 \sigma_i^x \sigma_{i+1}^x + g_2 \sigma_i^y \sigma_{i+1}^y)$ [33–37], and the dissipation is described by the Lindblad operator [38, 39] $\mathcal{D}(\rho) = \frac{\gamma}{2} \sum_{j=1, N} (2\sigma_j^z \rho \sigma_j^z - 2\rho)$. Let us choose $g_1, g_2 > 0$ and define $\lambda = g_2/g_1$. We consider this dissipation for its role directly to the edge modes as well as its exact solvability in some limiting cases. This model is fermionized using Majorana operators as $\alpha_{2j-1} = (\prod_k^{j-1} \sigma_k^z) \sigma_j^x, \alpha_{2j} = (\prod_k^{j-1} \sigma_k^z) \sigma_j^y$, after which [32, 40, 41]

$$H = ig_1 \sum_{j=1}^{N-1} \alpha_{2j} \alpha_{2j+1} - ig_2 \sum_{j=1}^{N-1} \alpha_{2j-1} \alpha_{2j+2}. \quad (2)$$

In this new basis the Lindblad operator is still localized: $\mathcal{D}(\rho) = -\gamma \sum_{j=1, N} (\alpha_{2j-1} \alpha_{2j} \rho \alpha_{2j-1} \alpha_{2j} + \rho)$ [42].

This dynamics respects the parity symmetry $[\mathcal{L}, P] = 0$ with $P = \prod_j^N \sigma_j^z = i^N \prod_j^{2N} \alpha_j$. In the long time limit,

$$\bar{\rho} = \lim_{t \rightarrow \infty} \rho(t) = (I + cP)/2^N, \quad (3)$$

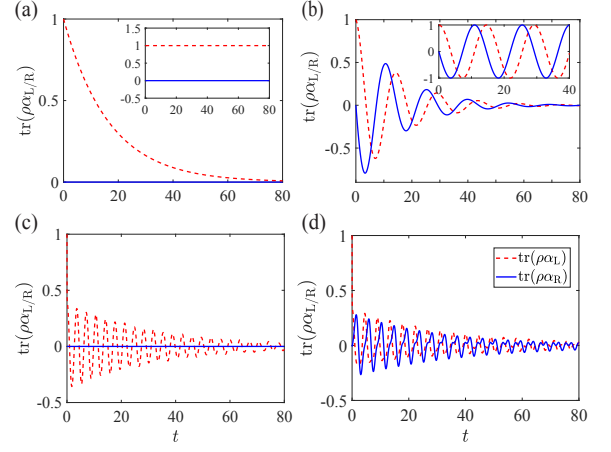


FIG. 3. Dynamics of $\text{tr}(\rho \alpha_{L/R})$ in fermion model. The parameters in these four subfigures are the same as Fig. 2.

where $c = \langle \Psi_0 | P | \Psi_0 \rangle$ is determined by the initial state.

This Hamiltonian supports two ferromagnetic phases polarized along either x ($\lambda < 1$) or y ($\lambda > 1$) directions (see Fig. 1 (b)), which correspond to the topological p -wave superconducting phases with opposite winding numbers after fermionization. The typical energy levels in the ferromagnetic phase are presented in Fig. 1 (a), in which the lowest two degenerate levels are separated from the bulk bands by a finite gap ε_g . These two states may be written as $|+\rangle^{\otimes N}$ and $|-\rangle^{\otimes N}$ in the small λ limit.

The spectra between the XY model and p -wave superconducting model are related by $E = \sum_i n_i \epsilon_i$, where $n_i = 0, 1$. In the fermion representation the energy levels are presented in Fig. 1 (c), with two localized MZMs at the open ends. This model can be regarded as two separate Majorana chains, that is, $A(\alpha_1, \alpha_4, \alpha_5, \dots)$ and $B(\alpha_2, \alpha_3, \alpha_6, \dots)$, as shown in Fig. 1 (d). We can bring Eq. 2 to a form of paired Majorana fermions [32, 43]

$$H = \frac{i}{2} \sum_{k=1}^{N-1} \epsilon_k b'_k b''_k + \frac{i \delta E_c}{2} \alpha_L \alpha_R, \quad (4)$$

where $\delta E_c = e^{-N/\xi} [(-1)^N + 1]$. Here α_L and α_R are edge zero modes at the left and right edges, which may be written as $\alpha_L = \alpha_1 - \lambda \alpha_5 + \lambda^2 \alpha_9 - \dots$ and $\alpha_R = \alpha_{2N} - \lambda \alpha_{2N-4} + \lambda^2 \alpha_{2N-8} - \dots$ (assuming $\lambda < 1$). We see that in an odd chain, the two edge modes reside on different subchains, which are fully decoupled; while for an even chain, they reside on the same chain and couple though the bulk in an exponential decaying way $e^{-N/\xi}$, where $\xi \propto 1/|\ln g_1 - \ln g_2|$ is the correlation length [32]. This odd-even effect is a typical feature of coupling between two distant MZMs, and the similar feature in two vortices can also be found [44]. In free space, it is changed to oscillation of coupling as a function of separation.

Evolution of the ground states. Let us first study the dynamics in a short chain investigated using exact nu-

merical method. In the fermion representation, we choose $|\Psi_0\rangle = (1 + \alpha_L)/\sqrt{2}|\text{vac}\rangle$ in the ground states manifold (hence $c = 0$ in Eq. 3), which has feature that $\alpha_L|\Psi_0\rangle = |\Psi_0\rangle$ and $\alpha_L(\alpha_R|\Psi_0\rangle) = -\alpha_R|\Psi_0\rangle$, thus $|\Psi_0\rangle$ and $\alpha_R|\Psi_0\rangle$ give the two edge modes. The numerical results for these two different models are presented in Figs. 2 and 3, respectively. In the weak dissipation limit when $\gamma \ll g_1, g_2$, the density matrix will exponentially approach the maximal mixed state $\bar{\rho} = I/2^N$ in an odd chain (see Eq. 3). However, in an even chain, it will decay to $\bar{\rho}$ with some oscillation with period determined by $T = 2\pi/\delta E_c$, where δE_c is the coupling between the two edge modes (see Eq. 4). This result indicates two thermalization channels in this model, that is, through the direct coupling between the edge modes and the coupling between the ground states manifold and excited bands. The latter channel is dominated when $N \gg \xi$.

The dynamics will become totally different in the strong dissipation limits (see (c) and (d) in Fig. 2 and Fig. 3), in which even when these two edge modes are decoupled exactly, oscillation of $\text{Tr}(\rho|i\rangle\langle i|)$ and $\text{Tr}(\rho\alpha_{L/R})$ can still be found. Now the dynamics is more complicated with some nonlinear oscillation. However, the final density matrix is still determined by $\bar{\rho}$. Strikingly, although the dissipation rate is increased by 400 times, much longer time for thermalization is required. In the short time dynamics, we find the XY model thermalizes much faster than the edge modes in Fig. 3 (c) and (d), due to reason that in the XY model, its ground states contain not only the edge modes, but also all the bulk modes (see Fig. 1 (a) and (c)).

It is necessary to point out that the dynamics restricted to the lowest two levels can not give rise to these dynamics. To this end, let us restrict the dynamics in these two levels. We can define $|1\rangle = |\Psi_0\rangle$ and $|2\rangle = \alpha_R|\Psi_0\rangle$, which satisfy $\langle i|\sigma_1^z|i\rangle = \langle i|\sigma_N^z|i\rangle = 0$ for $i = 1, 2$, then we obtain

$$\frac{d}{dt}\rho_{ii} = -\gamma(\rho_{ii} - \eta^2\rho_{i'i'}) - \gamma(\rho_{ii} - \eta^2\rho_{i'i'}), \quad (5)$$

where $\eta = \langle 1|\sigma_1^z|2\rangle = \langle 1|\sigma_N^z|2\rangle$ for $i \neq i'$, and η will decrease to zero exponentially with increasing of chain length. The evolution from this equation is shown in the inset of Fig. 2 (c), which decays exponentially to zero in a very short time. Thus although the lowest two states are separated from the bulk by a finite gap, the many-body dynamics need to take all excited states into account.

Dynamics of single fermion in the long time limit. To gain insight into the long time dynamics of ρ , we can write this matrix in term of Majorana fermions as

$$\rho = \frac{1}{2^N} \sum c_{a_1, a_2, \dots, a_{2N}} \alpha_1^{a_1} \alpha_2^{a_2} \dots \alpha_{2N}^{a_{2N}}, \quad (6)$$

where $a_j = 0, 1$. In this density matrix, only the first term with all $a_j = 0$ and the last term with all $a_j = 1$ is unchanged, which gives Eq. 3; while all the other terms will decay to zero in some way. In Fig. 4 (a), we plot

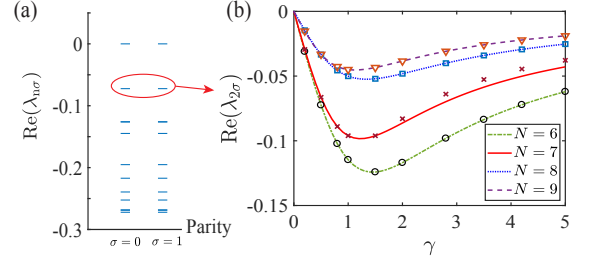


FIG. 4. (a) Eigenvalues $\text{Re}(\lambda_{n\sigma})$ of the superoperator \mathcal{L} in XY model in Eq. 1 (a). $\sigma = 0, 1$ accounts for the parity of P , and $N = 6$, $\gamma = 0.5$. (b) The lines are the largest imaginary part of eigenvalues from the non-Hermitian model in Eq. 7 and symbols are $\text{Re}(\lambda_{2\sigma})$ of \mathcal{L} . Other parameters are $g_1 = 1.0$ and $g_2 = 0.7$ in both subfigures.

the eigenvalues of the superoperator \mathcal{L} of the XY model, which have two zero eigenvalues, corresponding to parity symmetry. The different eigenvalues give different thermalization processes, thus the whole dynamics can not be described by a single exponential decaying function.

We can calculate the dynamics of single fermion by exploring the dynamics of $\text{tr}(\rho\alpha_n)$ via: $\frac{d}{dt}\text{tr}(\rho\alpha_n) = -i\text{tr}([H, \rho]\alpha_n) - \gamma \sum_{1,N} (\text{tr}(\alpha_{2j-1}\alpha_{2j}\rho\alpha_{2j-1}\alpha_{2j}) + \text{tr}(\rho\alpha_n))$. In the matrix form, we have [45]

$$i\frac{d}{dt}\Psi = 2(H_0 + i\Gamma)\Psi. \quad (7)$$

Here $\Psi = (\Psi_1, \Psi_4, \Psi_5, \dots)^T$ and $\Psi_i = \text{tr}(\rho\alpha_i)$, with α_i in chain A. H_0 is an antisymmetric matrix from the Hamiltonian of chain A, which is $H_A = -2i \sum_j (g_2\alpha_{4j-3}\alpha_{4j} - g_1\alpha_{4j}\alpha_{4j+1})$ and the dissipation matrix is given by $\Gamma = \text{diag}(-\gamma, 0, \dots, 0, -\gamma)$. In Fig. 4 (b) we plot the eigenvalues of the above non-Hermitian Hamiltonian, in which we find $\text{Re}(\lambda_{2\sigma})$ from superoperator \mathcal{L} and corresponding eigenvalue from Eq. 7 are consistent. These results indicate that while in the short time limit, the many-body thermalization is related to the many-body physics, in the long time limit, it is determined by the thermalization of the single particle modes.

Thermalization in the long chain limit. Two more issues need to be explained. (i) Why $\text{Re}(\lambda_{2\sigma})$ with $\sigma = 0, 1$ exhibit an inflexion point at finite γ ; and (ii) What will happen in the long chain limit? We consider the localized edge modes in chain A, while its treatment in chain B is similar. The eigenvalues in this tridiagonal bordered matrix are determined by [46–48]

$$\Delta_N = \frac{(g_1g_2)^{m-1}}{\sin\theta} [g_1g_2(2i\gamma + \epsilon)\sin(m+1)\theta + (-\gamma^2\epsilon + ig_1^2\gamma + ig_2^2\gamma)\sin(m\theta)] = 0, \quad (8)$$

when $N = 2m + 1$ is odd; and

$$\Delta_N = \frac{(g_1g_2)^{m-1}}{\sin\theta} [(-\gamma^2 + g_1^2 + i2\gamma\epsilon)\sin(m\theta) + g_1g_2\sin(m+1)\theta - \gamma^2\frac{g_2}{g_1}\sin(m-1)\theta] = 0, \quad (9)$$

when $N = 2m$ is even. In the above equations, ϵ is the eigenvalue and its relation to θ is determined by

$$\epsilon^2 = g_1^2 + g_2^2 + 2g_1g_2 \cos \theta. \quad (10)$$

When $\gamma = 0$, we have $\epsilon_n = \pm\sqrt{g_1^2 + g_2^2 + 2g_1g_2 \cos \theta_n}$ and $\theta_n = n\pi/(m+1)$ for $n = 0, \dots, N-1$. Thus the energy gap in Fig. 1 is given by $\epsilon_g = |g_1 - g_2|$.

The key observation is that in the long chain limit, the eigenvalues and the phase can be written as

$$\epsilon_n = \epsilon_{n,r} - i\epsilon_{n,i}, \quad \theta_n = \frac{n\pi}{m+1} + z_{n,r} + iz_{n,i}, \quad (11)$$

where $n \ll m$ and $\epsilon_{n,i}$, $z_{n,r}$, $z_{n,i}$ are small numbers in the sense that $\lim_{m \rightarrow \infty} m z_{n,i}/r = 0$ [49]. These solutions can be obtained by linearizing the above nonlinear equations.

(a) In the weak dissipation limit ($\gamma \ll g_1, g_2$) and in odd (o) and even (e) chains, we have

$$\epsilon_{n,i}^o = \frac{(g_1^2 + g_2^2)n^2\pi^2\gamma}{(g_1 + g_2)^2m^3}, \quad \epsilon_{n,i}^e = \frac{2g_2^2n^2\pi^2\gamma}{(g_1 + g_2)^2m^3}. \quad (12)$$

The expressions for $z_{n,r/i}$ can be found in Ref. [49]. The imaginary part of the eigenvalue is responsible for the thermalization, by which we can define a characteristic thermalization time T^* as,

$$T^* = \frac{1}{2\epsilon_{n,i}}. \quad (13)$$

When $\gamma = 0$, T^* is infinity, indicating of coherent dynamics from beginning to end. Since $\epsilon_{n,i} \propto \gamma$, it means that in the weak dissipation limit, thermalization is still important and can still happen in a finite system. Moreover, we find that the odd-even effect is still visible in the long chain limit.

(b) In the strong dissipation limit, the odd-even effect will vanish, and we find

$$\epsilon_{n,i} = \frac{2g_1^2g_2^2n^2\pi^2}{(g_1 + g_2)^2m^3\gamma}. \quad (14)$$

The expressions for $z_{n,r/i}$ can be found in Ref. [49]. We are surprised to find that in the strong dissipation limit, the thermalization time $T^* \propto \gamma N^3$, thus it will be prolonged by the dissipation. The crossover between these two cases are determined by $\epsilon_{n,i} = \epsilon_{n,i}^i$ with $i = e, o$, which yields $\gamma = g_1$ for even; while $\gamma = \sqrt{2}g_1g_2/\sqrt{g_1^2 + g_2^2}$ for odd. These inflexion points are also numerical verified, which are presented in Fig. 5 (b); see also Fig. 4 (b). No sudden changes of this inflexion point will happen even at the phase boundary $\lambda = 1$. The above solutions are also approximately correct even in the short chain in regarding of the fast decaying of imaginary part according to $\epsilon_{n,i} \propto 1/N^3$. With this expression, we find $T^* = 54$ in Fig. 2 (a) and $T^* = 80$ in Fig. 2 (c), which are qualitatively consistent with our observation.

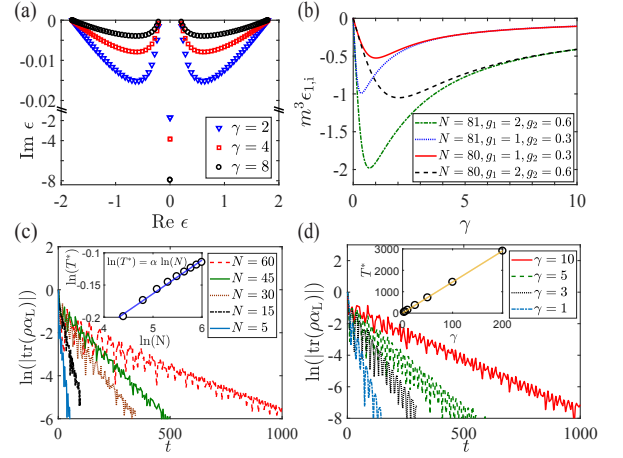


FIG. 5. (a) Spectra of the non-Hermitian matrix $H_0 + i\Gamma$ for $g_1 = 1, g_2 = 0.8, N = 80$ with different dissipation rate $\gamma = 2, 4, 8$. (b) $m^3 \epsilon_{1,i}$ as a function of γ for odd and even chains with chain length $N = 81$ and $N = 80$. (c) Long time evolution of $\text{tr}(\rho \alpha_L)$ for different chains with parameters $g_1 = 1, g_2 = 0.9, \gamma = 10$. Inset gives the scaling of thermalization time $\ln T^* = \alpha \ln N$, with fitted parameter $\alpha = 2.3$ in this time window. (d) Long time evolution of $\text{tr}(\rho \alpha_L)$ for different dissipation rates with parameters $g_1 = 1, g_2 = 0.95, N = 81$. Inset gives the scaling of thermalization time, with $T^* \propto \gamma$.

A general picture for these results. The above results are quite surprising. Let us try to understand these results using a simple picture based on perturbation theory. We come back to the non-Hermitian Schrödinger equation in (7), in which Ψ can be regarded as the wave function of a non-interacting tight-binding model with boundary dissipation. We can discuss the physics in two different limits in correspondence of the above two cases (a) and (b). When $\gamma \rightarrow 0$, we may treat the non-Hermitian term as perturbation, and to the leading term, we find $\epsilon_{n,i} \propto \langle \psi_n | i\Gamma | \psi_n \rangle \propto \gamma n^2 \pi^2 / N^3$, since the wave function density at the two end scales as $\rho \sim 2n^2 \pi^2 / N^3$. This feature can be understood at the special point $g_1 = g_2$ with corresponding wave function $|\psi_n\rangle = \sqrt{2/(N+1)} \sin\left(\frac{n\pi x}{N+1}\right)$. In the strong dissipation limit, we need to treat H_0 as perturbation. We need a second order perturbation theory by which we find $\epsilon_{n,i} \propto n^2 \pi^2 / \gamma N^3$. These results are consistent with the observation in Fig. 5 (c) and (d). Noticed that different energy levels, labeled by n , may have different thermalization time, and the state with $n = 1$ has the longest thermalization time, which may not be reached in Fig. 5 (c), thus in numerical simulation, we find $\ln T^* = \alpha \ln N$, with a prefactor $\alpha \sim 2.3$ in this particular case. The same picture is applicable even when several sites are dissipated near the boundaries. This result may have generality in the dynamics of many-body systems. In the weak dissipation limit, the first order contribution is dominated; while in the strong dissipation limit, the complex eigenvalues are weakly coupled to the real eigenvalues from second-order perturbation,

thus its effect can be suppressed. Moreover the scaling of $T^* \propto N^3$ comes from the overlap between the localized states and extended states, but not from the overlap between the two edge modes.

Conclusion. Dissipation in the many-body system is a fundamental problem that up to date has not yet been well understood. We explore the dissipation induced thermalization in a quantum XY model with boundary dissipation, in which the thermalization is characterized by a characteristic thermalization time T^* . We find that while any weak dissipation can induce thermalization with $T^* \propto 1/\gamma$, in the strong dissipation limit this process can be suppressed since $T^* \propto \gamma$. These counterintuitive results are explained by mapping the dynamics of single fermion density matrix to a non-Hermitian Hamiltonian. These results are useful for us to understand the dissipation dynamics of the topological qubits in coupling to the environment.

Acknowledgement. M.G. is supported by the National Youth Thousand Talents Program (No. KJ2030000001), the USTC start-up funding (No. KY2030000053) and the NSFC (No. GG2470000101). Z. Z. and G. G. are supported by National Key Research and Development Program (No. 2016YFA0301700), National Natural Science Foundation of China (No. 11574294), and the "Strategic Priority Research Program (B)" of the Chinese Academy of Sciences (No. XDB01030200).

* Email: gongm@ustc.edu.cn

† Email: zwzhou@ustc.edu.cn

- [1] Crispin W Gardiner and Hermann Haken, *Quantum noise*, Vol. 2 (Springer Berlin, 1991).
- [2] J Robert Johansson, Paul D Nation, and Franco Nori, "Qutip: An open-source python framework for the dynamics of open quantum systems," *Comput. Phys. Commun.* **183**, 1760–1772 (2012).
- [3] Hendrik Weimer, "Variational principle for steady states of dissipative quantum many-body systems," *Phys. Rev. Lett.* **114**, 040402 (2015).
- [4] Alexandre Le Boité, Giuliano Orso, and Cristiano Ciuti, "Steady-state phases and tunneling-induced instabilities in the driven dissipative bose-hubbard model," *Phys. Rev. Lett.* **110**, 233601 (2013).
- [5] Dragi Karevski, V Popkov, and GM Schütz, "Exact matrix product solution for the boundary-driven lindblad XXZ chain," *Phys. Rev. Lett.* **110**, 047201 (2013).
- [6] Tomaž Prosen, "Exact nonequilibrium steady state of an open hubbard chain," *Phys. Rev. Lett.* **112**, 030603 (2014).
- [7] Tomaž Prosen, "Exact nonequilibrium steady state of a strongly driven open XXZ chain," *Phys. Rev. Lett.* **107**, 137201 (2011).
- [8] Daniel A Rowlands and Austen Lamacraft, "Noisy spins and the richardson-gaudin model," *Phys. Rev. Lett.* **120**, 090401 (2018).
- [9] Leonardo Banchi, Daniel Burgarth, and Michael J Kastoryano, "Driven quantum dynamics: will it blend?" *Phys. Rev. X* **7**, 041015 (2017).
- [10] Mariya V Medvedyeva, Fabian HL Essler, and Tomaž Prosen, "Exact bethe ansatz spectrum of a tight-binding chain with dephasing noise," *Phys. Rev. Lett.* **117**, 137202 (2016).
- [11] Pedro Ribeiro and Tomaž Prosen, "Integrable quantum dynamics of open collective spin models," *Phys. Rev. Lett.* **122**, 010401 (2019).
- [12] In a many-body system, the dimension of the Hilbert $\text{Dim}(H)$ space increases exponentially with the size of the system. However, the dimension of the density matrix for the mixed space in open systems should be $\text{Dim}(H)^2$.
- [13] Jens Eisert, Mathis Friesdorf, and Christian Gogolin, "Quantum many-body systems out of equilibrium," *Nat. Phys.* **11**, 124 (2015).
- [14] Rahul Nandkishore and David A Huse, "Many-body localization and thermalization in quantum statistical mechanics," *Annu. Rev. Condens. Matter Phys.* **6**, 15–38 (2015).
- [15] Hannes Bernien, Sylvain Schwartz, Alexander Keesling, Harry Levine, Ahmed Omran, Hannes Pichler, Soonwon Choi, Alexander S Zibrov, Manuel Endres, Markus Greiner, *et al.*, "Probing many-body dynamics on a 51-atom quantum simulator," *Nature* **551**, 579 (2017).
- [16] CJ Turner, AA Michailidis, DA Abanin, M Serbyn, and Z Papić, "Weak ergodicity breaking from quantum many-body scars," *Nat. Phys.* **14**, 745 (2018).
- [17] CJ Turner, AA Michailidis, DA Abanin, M Serbyn, and Z Papić, "Quantum scarred eigenstates in a rydberg atom chain: Entanglement, breakdown of thermalization, and stability to perturbations," *Phys. Rev. B* **98**, 155134 (2018).
- [18] Chetan Nayak, Steven H Simon, Ady Stern, Michael Freedman, and Sankar Das Sarma, "Non-abelian anyons and topological quantum computation," *Rev. Mod. Phys.* **80**, 1083 (2008).
- [19] Michael Freedman, Alexei Kitaev, Michael Larsen, and Zhenghan Wang, "Topological quantum computation," *Bull. Amer. Math. Soc.* **40**, 31–38 (2003).
- [20] Jay D Sau, Roman M Lutchyn, Sumanta Tewari, and S Das Sarma, "Generic new platform for topological quantum computation using semiconductor heterostructures," *Phys. Rev. Lett.* **104**, 040502 (2010).
- [21] Hao Zhang, Chun-Xiao Liu, Sasa Gazibegovic, Di Xu, John A Logan, Guanzhong Wang, Nick Van Loo, Jouri DS Bommer, Michiel WA De Moor, Diana Car, *et al.*, "Quantized majorana conductance," *Nature* **556**, 74 (2018).
- [22] Stevan Nadj-Perge, Ilya K Drozdov, Jian Li, Hua Chen, Sangjun Jeon, Jungpil Seo, Allan H MacDonald, B Andrei Bernevig, and Ali Yazdani, "Observation of majorana fermions in ferromagnetic atomic chains on a superconductor," *Science*, 1259327 (2014).
- [23] Dongfei Wang, Lingyuan Kong, Peng Fan, Hui Chen, Shiyu Zhu, Wenya Liu, Lu Cao, Yujie Sun, Shixuan Du, John Schneeloch, *et al.*, "Evidence for majorana bound states in an iron-based superconductor," *Science* **362**, 333–335 (2018).
- [24] Hao-Hua Sun, Kai-Wen Zhang, Lun-Hui Hu, Chuang Li, Guan-Yong Wang, Hai-Yang Ma, Zhu-An Xu, Chun-Lei Gao, Dan-Dan Guan, Yao-Yi Li, *et al.*, "Majorana zero mode detected with spin selective andreev reflection in the vortex of a topological superconductor," *Phys. Rev. Lett.* **116**, 257003 (2016).

- [25] Jin-Peng Xu, Mei-Xiao Wang, Zhi Long Liu, Jian-Feng Ge, Xiaojun Yang, Canhua Liu, Zhu An Xu, Dandan Guan, Chun Lei Gao, Dong Qian, *et al.*, “Experimental detection of a majorana mode in the core of a magnetic vortex inside a topological insulator-superconductor $\text{Bi}_2\text{Te}_3/\text{NbSe}_2$ heterostructure,” *Phys. Rev. Lett.* **114**, 017001 (2015).
- [26] Qin Liu, Chen Chen, Tong Zhang, Rui Peng, Ya-Jun Yan, Xia Lou, Yu-Long Huang, Jin-Peng Tian, Xiao-Li Dong, Guang-Wei Wang, *et al.*, “Robust and clean majorana zero mode in the vortex core of high-temperature superconductor $(\text{Li}_{0.84}\text{Fe}_{0.16})\text{OHFeSe}$,” *Phys. Rev. X* **8**, 041056 (2018).
- [27] Vincent Mourik, Kun Zuo, Sergey M Frolov, SR Plissard, Erik PAM Bakkers, and Leo P Kouwenhoven, “Signatures of majorana fermions in hybrid superconductor-semiconductor nanowire devices,” *Science* **336**, 1003–1007 (2012).
- [28] MT Deng, CL Yu, GY Huang, Marcus Larsson, Philippe Caroff, and HQ Xu, “Anomalous zero-bias conductance peak in a Nb-InSb Nanowire-Nb hybrid device,” *Nano Lett.* **12**, 6414–6419 (2012).
- [29] Anindya Das, Yuval Ronen, Yonatan Most, Yuval Oreg, Moty Heiblum, and Hadas Shtrikman, “Zero-bias peaks and splitting in an Al-InAs nanowire topological superconductor as a signature of majorana fermions,” *Nat. Phys.* **8**, 887 (2012).
- [30] RM Lutchyn, EPAM Bakkers, LP Kouwenhoven, P Krogstrup, CM Marcus, and Y Oreg, “Majorana zero modes in superconductor-semiconductor heterostructures,” *Nat. Rev. Mater.* **3**, 52 (2018).
- [31] Jason Alicea, “New directions in the pursuit of majorana fermions in solid state systems,” *Rep. Prog. Phys.* **75**, 076501 (2012).
- [32] A Yu Kitaev, “Unpaired majorana fermions in quantum wires,” *Physics-Uspekhi* **44**, 131 (2001).
- [33] Andreas Osterloh, Luigi Amico, Giuseppe Falci, and Rosario Fazio, “Scaling of entanglement close to a quantum phase transition,” *Nature* **416**, 608 (2002).
- [34] Shi-Liang Zhu, “Scaling of geometric phases close to the quantum phase transition in the XY spin chain,” *Phys. Rev. Lett.* **96**, 077206 (2006).
- [35] Jens Eisert and Tobias J Osborne, “General entanglement scaling laws from time evolution,” *Phys. Rev. Lett.* **97**, 150404 (2006).
- [36] Tobias J Osborne and Michael A Nielsen, “Entanglement in a simple quantum phase transition,” *Phys. Rev. A* **66**, 032110 (2002).
- [37] Jia-Ming Cheng, Ming Gong, Guang-Can Guo, and Zheng-Wei Zhou, “Scaling of geometric phase and fidelity susceptibility across the critical points and their relations,” *Phys. Rev. A* **95**, 062117 (2017).
- [38] M Hein, W Dür, and H-J Briegel, “Entanglement properties of multipartite entangled states under the influence of decoherence,” *Phys. Rev. A* **71**, 032350 (2005).
- [39] Jian-Ming Cai, Zheng-Wei Zhou, and Guang-Can Guo, “Decoherence effects on the quantum spin channels,” *Phys. Rev. A* **74**, 022328 (2006).
- [40] Eugene P. Wigner Pascual Jordan, “About the pauli exclusion principle,” *Z. Phys.* **47**, 631 (1928).
- [41] Subir Sachdev, *Quantum phase transitions* (Cambridge university press, 2011).
- [42] This dissipation term written in canonical fermion representation is $\mathcal{D}(\rho) = -\gamma \sum_{j=1,N} (4c_j^\dagger c_j \rho c_j^\dagger c_j - 2c_j^\dagger c_j \rho - 2\rho c_j^\dagger c_j + 2\rho)$, where $c_1 = \alpha_1 + i\alpha_2$ and $c_N = \alpha_{2N-1} + i\alpha_{2N}$.
- [43] Alexei Kitaev and Christopher Laumann, “Topological phases and quantum computation,” *Les Houches Summer School Exact methods in low-dimensional physics and quantum computing* **89**, 101 (2009).
- [44] Meng Cheng, Roman M Lutchyn, Victor Galitski, and S Das Sarma, “Splitting of majorana-fermion modes due to intervortex tunneling in a $p_x + ip_y$ superconductor,” *Phys. Rev. Lett.* **103**, 107001 (2009).
- [45] When the total number is conserved, one may finds that $\text{Tr}(\rho\alpha_i) = 0$. However, in a dissipative system, the total number is not conserved, thus this quantity is nonzero. It will yield some useful information to the dynamics of the density matrix, though not all of it.
- [46] Said Kouachi, “Eigenvalues and eigenvectors of tridiagonal matrices,” *Electronic Journal of Linear Algebra* **15**, 8 (2006).
- [47] Wen-Chyuan Yueh, “Eigenvalues of several tridiagonal matrices,” *Applied mathematics e-notes* **5**, 210–230 (2005).
- [48] Allan R Willms, “Analytic results for the eigenvalues of certain tridiagonal matrices,” *SIAM Journal on Matrix Analysis and Applications* **30**, 639–656 (2008).
- [49] In the weak dissipation limit ($\gamma \ll g_1, g_2$), we obtain $z_{n,r} = -(\pi\gamma^2 n(g_1 g_2 - g_1^2 - g_2^2))/(g_1^2 g_2^2 m^2)$ and $z_{n,i} = ((g_1^2 + g_2^2)\pi\gamma n)/(g_1 g_2 (g_1 + g_2) m^2)$ for $N = 2m + 1$. When $N = 2m$, these two expressions will become $z_{n,r} = (g_2 n \pi (g_1^2 - 2\gamma^2))/(g_1^2 m^2 (g_1 + g_2))$ and $z_{n,i} = 2g_2 \pi \gamma n/(g_1 (g_1 + g_2) m^2)$. In the strong dissipation limit ($\gamma \gg g_1, g_2$), we obtain some different expressions. When $N = 2m + 1$, $z_{n,r} = \pi n/m^2 - \pi g_1 g_2 n/(\gamma^2 m^2)$, and $z_{n,i} = 2\pi g_1 g_2 n/(\gamma m^2 (g_1 + g_2))$; and for $N = 2m$, we find $z_{n,r} = (2g_2 g_1^2 n \pi)/(\gamma^2 m^2 (g_1 + g_2)) - (g_2 n \pi)/(m^2 (g_1 + g_2))$ and $z_{n,i} = 2g_1 g_2 n \pi/(\gamma m^2 (g_1 + g_2))$. The expression for $\epsilon_{n,i}$ can be deduced from $z_{n,i,r}$. In all these expressions, we find $\lim_{m \rightarrow \infty} m z_{n,i/r} = 0$, which is the basic assumption in solving of the nonlinear equation $\Delta_N = 0$.